Jpn. J. Cancer Res. **92**, 989–995, September 2001

Pharmacokinetic Study of a Gallium-porphyrin Photo- and Sono-sensitizer, ATX-70, in Tumor-bearing Mice

Kazuaki Sasaki,[1] Nagahiko Yumita,[2,5] Ryuichiro Nishigaki,[2] Isao Sakata,[3] Susumu Nakajima[4] and Shin-ichiro Umemura[1]

[1]Central Research Laboratory, Hitachi, Ltd., 1-280 Higashi-Koigakubo, Kokubunji, Tokyo 185-8601, [2]School of Pharmaceutical Science, Toho University, 2-2-1 Miyama, Funabashi, Chiba 272-8510, [3]Photochemical Co., Ltd., 5319-1 Haga, Okayama 701-1221 and [4]Obihiro University of Agriculture and Veterinary Medicine, Inada-cho, Obihiro, Hokkaido 080-8555

The tissue distribution of a gallium-porphyrin photo- and sono-sensitizer, 7,12-bis(1-decyloxyethyl)-Ga(III)-3,8,13,17-tetramethylporphyrin-2,18-dipropionyldiaspartic acid, ATX-70, was pharmacokinetically examined in tumor-bearing mice. The drug was administered intravenously to CDF_1 mice implanted with Colon 26 carcinoma. Blood and tissue samples were collected for up to 72 h after administration. The drug concentration was determined by high-performance liquid chromatography (HPLC) with fluorescence detection. ATX-70 was found to accumulate in tumors at a relatively high concentration that peaked between 2 h and 6 h after administration. However, modest concentrations of ATX-70 also remained in healthy tissues for up to 6 h. We examined the distribution of ATX-70 in the tumor in comparison with other tissues from the viewpoint of minimizing possible side effects of laser or ultrasound exposure while maintaining the treatment effect. About 24 h after administration, the tumor/plasma concentration ratio peaked, and relatively high tumor/skin and tumor/muscle concentration ratios were seen.

Key words: ATX-70 — Pharmacokinetics — Colon 26 — Sonodynamic therapy — Photodynamic therapy

Several investigators have studied the utility of porphyrins as agents to localize malignant tissues. Such chemicals were found to have therapeutic efficacy against human malignancies in a treatment regimen currently termed photodynamic therapy (PDT).[1,2] The technique involves the systemic administration of tumor-localizing photosensitizers and their subsequent excitation with visible light to produce tumor necrosis.

Yumita *et al.* have demonstrated that hematoporphyrin (Hp), a photochemical sensitizer whose derivatives (HpD) are known to be useful for PDT, also induces significant cell damage when activated with ultrasound.[3] It was demonstrated that Hp has potential to be used as a sonochemical sensitizer for tumor treatment in combination with ultrasound, in what may be referred to as sonodynamic therapy (SDT).[4–6] It was of interest to study whether other photosensitizers may be activated not only photochemically, but also sonochemically.

Among the metal-deuteroporphyrin complexes, which had been synthesized as photosensitizers for photodynamic therapy, the gallium complexes showed the longest phosphorescence lifetime—much longer than Hp or HpD.[7] This long phosphorescence lifetime can be a great advantage in the efficient generation of singlet oxygen. Among these gallium complexes, 7,12-bis(1-decyloxyethyl)-Ga(III)-3,8,13,17-tetramethylporphyrin-2,18-dipropionyldiaspartic acid, referred to as ATX-70 (Fig. 1), was found to induce significant tumor tissue destruction in combination with pulsed laser irradiation.[7] This suggests that ATX-70 has potential as a photosensitizer for photodynamic therapy.

Umemura *et al.* investigated the enhancement of ultrasonically induced cell damage by ATX-70.[8] The rate of cell damage of isolated sarcoma 180 cells in air-saturated suspensions was more than four times higher than when ultrasound was used alone, and more than two times higher than when it was used with Hp under the same exposure conditions. This result suggests that ATX-70 might be a better sensitizer than Hp for ultrasound tumor treatment.

PDT of cancer is based on the use of photosensitizing agents that concentrate relatively selectively in tumors and become cytotoxic when activated by light at the appropriate wavelength. Similarly the localization of the cytotoxic effect induced by SDT to the treated tumor comes from focusing the ultrasound energy on the targeted area and from tumor-selective localization of sensitizers for SDT. The distribution of these agents not only in tumors, but also in healthy tissues may lead to unwanted effects due to PDT- or SDT-induced damage to other organs. Because detailed analysis of the tissue distribution of the drug may allow us to determine the appropriate timing for the exposure to light or ultrasound after administration when significant tumor necrosis can be achieved without major

[5] To whom correspondence should be addressed.
E-mail: nagahiko@phar.toho-u.ac.jp

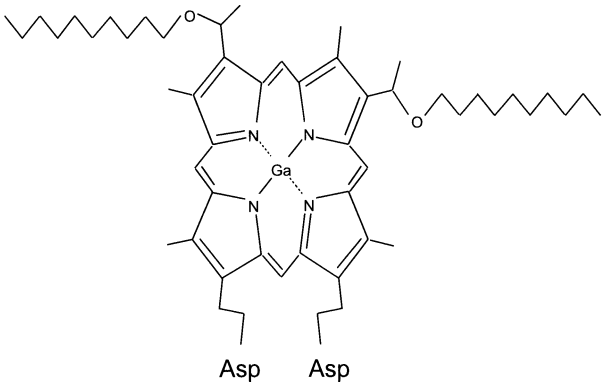

Fig. 1. Chemical structure of gallium-porphyrin complex, ATX-70. ASP: aspartic acid.

detrimental effects to healthy tissues, the concentrations of drugs in tumor tissue as well as normal tissues have been studied by many researchers.[9, 10)]

Because the tissue distribution of ATX-70 has not been clearly investigated, we measured the concentration of ATX-70 in the plasma and in several tissues including a tumor subcutaneously implanted in mice. We analyzed the distribution of ATX-70 in the tumor-bearing mice and calculated the pharmacokinetic parameters.

MATERIALS AND METHODS

Materials ATX-70 was supplied by Toyo Hakka Kogyo (Okayama). All other reagents were commercial products of analytical grade.

Tumor cells and animals Colon 26 carcinoma was supplied by the Cancer Institute (Tokyo). The cells were passaged weekly through male BALB/c mice (5 weeks old). Transplanted tumors were initiated by subcutaneous trocar-injection of approximately 1-mm^3 pieces of fresh tumor into the left dorsal scapula region of male 5-week-old CDF_1 mice. When the tumor reached a diameter of about 10−12 mm approximately 14 days after implantation, the pharmacokinetic study was started.

Determination of ATX-70 concentration in blood and tissue ATX-70 was dissolved in a sterilized saline solution and administered to tumor-bearing CDF_1 mice at a dose of 2.5 mg/kg by intravenous injection from the caudal vein. This dose of the drug has been shown to induce an anti-tumor effect on subcutaneously implanted murine Colon 26 in combination with ultrasound 24 h after administration.[11)] Under pentobarbital anesthesia, blood samples were obtained by heart puncture 1, 2, 6, 12, 24, 48, and 72 h after injection. Immediately after the blood sampling, the blood was placed in a heparin-coated test tube and centrifuged at 2500*g* for 10 min to separate the plasma. The tumor, liver, spleen, kidney, lung, heart, muscle and skin were taken immediately after killing of the animals at 2, 6, 24, 48, and 72 h after injection. The tissues were excised, blotted dry and weighed. Samples were stored at −20°C until used. Plasma (0. 1 ml) was mixed with 2.4 ml of 100 m*M* citric acid buffer (pH 3.0). A portion of tissue (0.1 g) was homogenized in 4.0 ml of the same buffer. Then 2.5 ml of plasma-buffer sample and the 2.5 ml of tissue homogenate were each extracted with 5.0 ml of a chloroform:methanol mixture (1:1, v/v). After centrifugation at 3000*g* for 10 min, the chloroform layer was removed. The aqueous layer was shaken with 2.5 ml of chloroform for the second extraction. The first and the second chloroform layers were combined and evaporated to dryness in a water bath at 40°C. The residue was dissolved in 1.0 ml of a mobile phase for high-performance liquid chromatography (HPLC). After centrifugation at 2500*g* for 5 min, a 5-μl portion of the supernatant was injected into an HPLC system consisting of a pump (model L-6200, Hitachi, Tokyo), a fixed-loop injector (model 7125, Rheodine, Cotani, CA), an analytical column (Wakocil 5C8, Wako Pure Chemical Ind., Osaka), a fluorescence detector (model F-1000, Hitachi, excitation: 405 nm, emission: 570 nm) and a data processor (model D-2500, Hitachi). The mobile phase was a mixture of methanol, water, and acetic acid (85:5:10, v/v/v). The flow rate was 1.2 ml/min. HPLC was used for the assay of ATX-70 because it provides the sensitivity required to quantify this potent drug, combined with a high degree of specificity. Extraction and chromatography of drug-free tissues resulted in chromatographic traces free of interfering peaks at the ATX-70 retention times. An assay using only batch fluorescence, for example, would have overestimated the concentration of ATX-70, particularly for samples containing unknown fluorescent materials, which eluted close to the void volume of the column.

Plasma protein binding and blood-to-plasma partition coefficient (R_B) Plasma protein binding of ATX-70 was examined with the use of an ultrafiltration kit (Centrifree micropartition system, Amicon, Grace Japan, Tokyo). We added 50 μl of the solution containing ATX-70 (1.0 mg/ml) to 950 μl of the plasma collected from each CDF_1 mouse, mixed the 1.0-ml sample, and stored it at 37°C for 5 min to ensure complete binding equilibrium. Immediately after ultrafiltration of the sample by centrifugation at 2000*g* for 5 min, 20 μl of the ultrafiltrate was injected into the HPLC system to determine the unbound concentration of ATX-70. The ratio of the ATX-70-bound fraction was calculated according to the equation

$$f_{bound}=(C_{total}-C_{free})/C_{total},$$

where f_{bound}, C_{free}, and C_{total} are the ratio of the ATX-70-bound fraction, the concentration of ATX-70-unbound fraction (determined from HPLC) in the filtrate, and the total ATX-70 concentration in plasma, respectively.

The R_B was also measured *in vivo*. Blood samples (500 μl) were collected 2 h after intravenous administration of ATX-70 at a dose of 5 mg/kg. Each blood sample was divided into two parts. One part was centrifuged at 2500*g* for 10 min to separate the plasma. The plasma and 100 μl of the second part of the blood sample were each mixed with 2.4 ml of 100 m*M* citric acid buffer (pH 3.0) for HPLC measurement. The value of R_B was calculated according to the equation

$$R_B = C_{blood}/C_{plasma},$$

where C_{blood} and C_{plasma} are the ATX-70 concentrations in blood and in plasma, respectively.

Pharmacokinetic analysis Pharmacokinetic analysis of the disappearance of ATX-70 from the plasma was done based on a two-compartment open model. The plasma concentration of ATX-70 ($C_P(t)$) is described by Eq. 1. The observed plasma concentrations were fitted to Eq. 1 and pharmacokinetic parameters, A, α, B, and β were determined by means of a non-linear least-squares method.

$$C_P(t) = A\exp(-\alpha t) + B\exp(-\beta t) \quad (1)$$

The area under the plasma concentration curve (AUC) from time zero to infinity, the plasma total body clearance (Cl_{tot}), and the distribution volume at the steady state (V_{dss}) are given by the equations

$$AUC = A/\alpha + B/\beta, \quad (2)$$

$$Cl_{tot} = \text{dose}/AUC, \quad (3)$$

$$V_{dss} = \text{dose}\,(A\beta^2 + B\alpha^2)/(B\alpha + A\beta)^2. \quad (4)$$

In the rapid equilibrium condition for ATX-70 between the plasma and the tissue, the concentration of ATX-70 in the tissue ($C_T(t)$) can be expressed as the convolution form

$$C_T(t) = \int_0^t R_B \cdot C_P(t-\theta) \cdot W(\theta)\, d\theta, \quad (5)$$

where $W(t)$ is the Laplace antitransform of the transfer function which describes the transfer of drug from the plasma into the tissue. In general, $W(t)$ is expressed in a multi-exponential form as

$$W(t) = \sum_{n=1}^{N} K_{2n-1}\exp(-K_{2n}t), \quad (6)$$

where K_{2n-1} and K_{2n} are first-order rate constants. Substitution of Eqs. 1 and 6 into Eq. 5 gives

$$C_T(t) = R_B \sum_{n=1}^{N} K_{2n-1}\,[\{A\{\exp(-\alpha t) - \exp(-K_{2n}t)\}/(K_{2n} - \alpha) + B\,\{\exp(-\beta t) - \exp(-K_{2n}t)\}/(K_{2n} - \beta)]. \quad (7)$$

The tissue concentration curves of ATX-70 were fitted to Eq. 7, and the number of exponential terms in Eq. 6, N was assessed by the use of Akaike's information criterion.[12] They were best expressed with two exponential terms (N=2). Thus, K_1, K_2, K_3, and K_4 for each tissue were obtained by fitting the observed tissue concentration to the equation

$$C_T(t) = R_B[K_1A\{\exp(-\alpha t) - \exp(-K_2t)\}/(K_2 - \alpha) + K_1B\{\exp(-\beta t) - \exp(-K_2t)\}/(K_2 - \beta) + K_3A\{\exp(-\alpha t) - \exp(-K_4t)\}/(K_4 - \alpha) + K_3B\{\exp(-\beta t) - \exp(-K_4t)\}/(K_4 - \beta)], \quad (8)$$

with the nonlinear least-squares method. Concentration ratios between different tissues were calculated from these fitted values.

The tissue-to-blood concentration ratio (K_B) was calculated from the following equation

$$K_B = C_T(t)/C_P(t)/R_B. \quad (9)$$

This can be expressed as,

$$K_B = K_1/K_2 + K_3/K_4. \quad (10)$$

In this paper, we use Eq. 10 for each tissue.

RESULTS

The concentration of ATX-70 in the plasma after intravenous administration is shown in Fig. 2.[11] The observed data were best fitted to a bi-exponential equation, and the calculated pharmacokinetic parameters are listed in Table I.[11] The elimination half-life at the terminal phase ($t_{1/2}$) was 25 h. The distribution volume (V_{dss}) was 71.6 ml/kg. The R_B was 0.56±0.06.

The time courses of ATX-70 concentration in the tissues are shown in Fig. 3. The parameters reflecting the tissue distribution, calculated with Eq. 2 using the observed data and the parameters in Table I, are listed in Table II. The fitting curves for the concentrations in tissues shown in Fig. 3 were calculated with Eq. 5 and the parameters listed in Table II. The concentrations of ATX-70 in all tissues were well predicted.

In the tumor there was an obvious rising phase: the ATX-70 concentration peaked between 2 h and 6 h. The

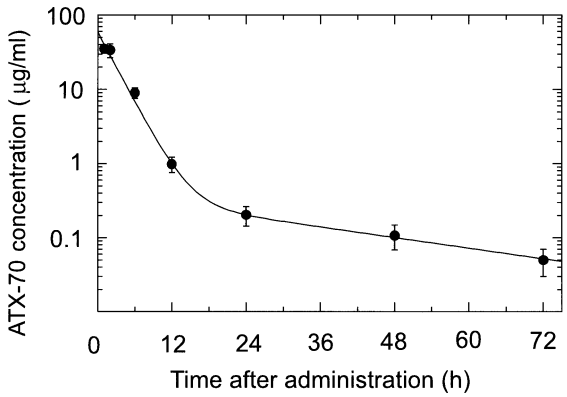

Fig. 2. Time course of ATX-70 in plasma after administration of the drug at the dose of 2.5 mg/kg. The points represent the mean±SD of four mice.

Table I. Pharmacokinetic Parameters of ATX-70 after Intravenous Administration

Parameter[a)]	Value
A (μg/ml)	61.5
α (h^{-1})	0.362
B (μg/ml)	0.379
β (h^{-1})	0.0277
AUC (μg h/ml)	183
Cl_{tot} (ml/h/kg)	13.6
V_{dss} (ml/kg)	71.6

a) Parameters were calculated from the mean plasma concentrations of four mice.

peak concentration in the liver was about 5–10 times higher than in other tissues. The peak concentration in the liver occurred between 6 h and 12 h. High concentrations were observed in the kidney, lung, spleen, and heart but no obvious increase of the concentrations was seen. Although the peak concentrations in the skin and muscle were very low compared with other tissues, the decay of the concentrations was very slow.

The K_B, also listed in Table II, indicate the distribution of the drug between tissues and blood. The K_B value for tumor was approximately three times the values for skin and muscle.

The fitted tumor/plasma, tumor/skin, and tumor/muscle concentration ratios after administration are plotted in Fig. 4. The tumor/muscle ratio rose during the first 6 h then declined. The tumor/skin ratio rose during the first 3 h, slightly decreased, then remained constant after 12 h. The tumor/plasma ratio rose and reached a peak at 24 h, then declined very slowly.

We also determined the plasma protein binding ratio of ATX-70. The binding ratio was calculated from the total amount of ATX-70 and the amount of unbound ATX-70 determined by HPLC. ATX-70 was highly bound to the plasma protein: the mean ratio of protein binding was 99.8±0.1%.

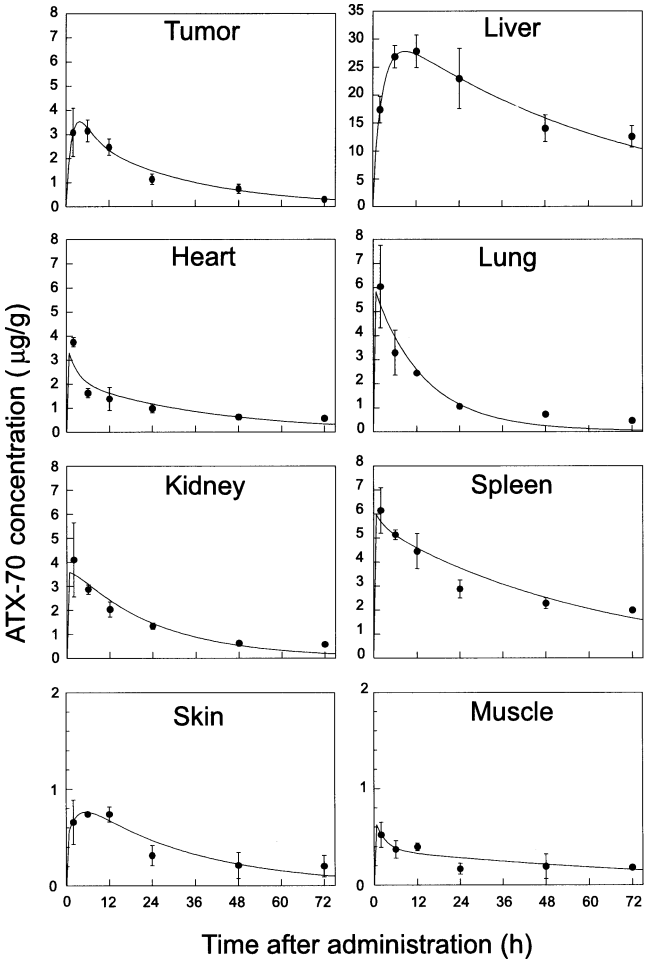

Fig. 3. Time course of ATX-70 in various tissues after administration of the drug. The dose was 2.5 mg/kg. The points represent the mean±SD of four mice.

DISCUSSION

As shown in Fig. 3, the concentration of ATX-70 in the tumor gradually increased and reached a peak about 6 h after administration. The peak ATX-70 concentration was 3.5 μg/g, which represents a relatively high accumulation in the tumor. Many researchers have reported that low-density lipoprotein (LDL) binds to porphyrins in plasma[13, 14] and plays a role in the accumulation of porphyrins by tumor tissues.[15] It is thought that rapidly growing tumors and tissues have a high density of lipoprotein receptors and acquire the lipids needed for membrane synthesis either through non-specific endocytosis or through receptor-mediated endocytosis of LDL.[16, 17] In this experiment, the *in vitro* plasma protein binding ratio of ATX-70 was more than 99.7%. LDL is a candidate protein to bind ATX-70 in plasma, so the accumulation of ATX-70 in the tumor may be mediated by an LDL pathway. As shown in Fig. 3, ATX-70 accumulates particularly in the liver. The K_B values of ATX-70 for the liver and spleen (Table II) were 10.9 and 3.28, respectively, showing that ATX-70 has the highest affinity to the liver and a relatively high affinity to the spleen in comparison with other tissues. Bellnier *et al.* reported that large amounts of Photofrin II were distributed in the liver and spleen,[10] which are rich in reticuloendothelial components. Since the liver and spleen are highly active sites of lipoprotein catabolism,[16] LDL is likely to efficiently deliver ATX-70 to the liver and spleen. However, we did not determine whether LDL

Table II. Parameters Reflecting the Tissue Distribution Calculated by Eq. 2 Using the Observed Data and the Parameters in Table I

Tissue	K_1 (min^{-1})	K_2 (min^{-1})	K_3 ($\times 10^{-4}$ min^{-1})	K_4 ($\times 10^{-4}$ min^{-1})	K_B ($K_1/K_2+K_3/K_4$)
Liver	0.846	5.46	52.7	4.92	10.9
Kidney	2.35	22.2	6.33	7.57	0.941
Heart	2.95	27.1	3.59	4.68	0.876
Lung	36.5	201	8.46	12.1	0.887
Skin	0.130	7.69	1.60	5.52	0.303
Muscle	0.0501	2.40	0.625	2.11	0.318
Tumor	0.0567	0.733	6.63	7.53	0.957
Spleen	0.500	2.76	9.37	3.02	3.28

could bind ATX-70 in plasma, so further investigation is needed to determine how ATX-70 accumulates in plasma and is delivered to the tumor.

ATX-70 significantly accumulates in the tumor up to 6 h after administration (Fig. 3). However, ATX-70 also remains in other tissues at modest concentration levels for up to 6 h (Fig. 3). Therefore, 6 h or less after administration is unlikely to be the best time for laser exposure or ultrasound exposure because unwanted effects in non-targeted organs are possible. In most PDT with HPD, laser exposure is done 24–48 h after the administration of HPD to avoid side effects, even though the concentration of HPD in a tumor is likely to peak within a few hours.[2] Thus, the ratio of ATX-70 accumulation in the tumor to that in other tissues is important in order to maximize the treatment effect while suppressing side effects.

The highest tumor/tissue concentration ratios for skin and muscle are seen 3–6 h after administration (Fig. 4). The concentration in the tumor was approximately four and eight times that in skin and in muscle respectively, during that period. However, the tumor/plasma concentration ratio was less than 1.0 up to 6 h after administration. Laser or ultrasound exposure 3–6 h after ATX-70 administration might cause vascular damage in non-targeted organs. On the other hand, the ATX-70 concentration in the tumor was at least three times the concentration in skin, muscle, and plasma between 12 h and 48 h after injection. This is likely to be favorable for preventing side effects.

The tumor/plasma concentration ratio peaked about 24 h after administration, and relatively high tumor/skin and tumor/muscle concentration ratios were also observed at that time, as shown in Fig. 4. The concentration in tumors 24 h after administration, measured by HPLC, was 1.15 ± 0.23 μg/g in our study. We have already reported that significant anti-tumor activity against subcutaneously implanted Colon 26 carcinoma was induced by ultrasound exposure when ATX-70 was injected 24 h before the exposure.[11] This report suggested that the ATX-70 concentration in a tumor 24 h after administration was high enough to generate an ultrasound-induced anti-tumor effect.

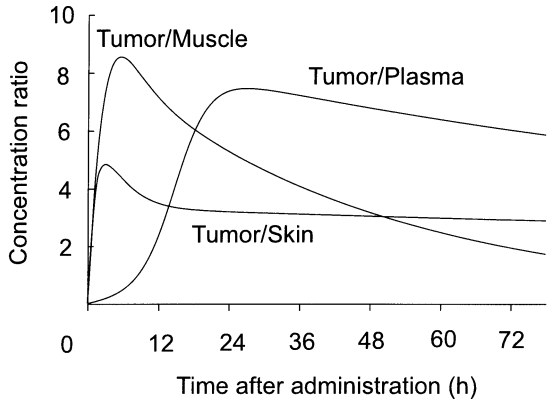

Fig. 4. Tumor/tissue concentration ratios corresponding to the fitted values: tumor/plasma, tumor/skin, and tumor/muscle were plotted.

In the PDT of cancer, photosensitizing agents are expected to be concentrated relatively selectively in tumors and to become cytotoxic only when activated by light. Similarly the localization of the cytotoxic effect induced by SDT to the treated tumor is achieved by focusing the ultrasound energy on the target area and by selective localization of the sensitizing agents for SDT. Focused ultrasound can penetrate much deeper into tissues than light can. This is advantageous for using focused ultrasound for selectively treating non-superficial tumors in combination with an SDT sensitizer. We emphasize, however, that the distribution of these agents in normal tissues, as well as in tumors, may lead to SDT-induced damage to other organs. As shown in Fig. 4, the highest tumor/plasma ratio was observed around 24 h after ATX-70 administration and relatively high tumor/skin and tumor/muscle concentration ratios were also observed at that time in subcutaneous tumor-bearing mice. The time point of 24 h after administration is likely to be the best time for ultrasound exposure. We also reported that the growth of Walker 256 tumors implanted in rat kidneys was significantly suppressed by focused ultrasound when ATX-70

was injected 24 h before exposure.[18] In this report, the concentration of ATX-70 accumulated in the implanted Walker 256 tumor tissue was one order of magnitude higher than that in the plasma 24 h after administration. The concentration was about twice as high as that in the surrounding normal kidney tissue on average at 24 h after administration. This tendency of ATX-70 to accumulate in tumor tissue should be advantageous for localizing the ultrasonically induced effect of ATX-70.

Recently, Jin *et al.* investigated the combination effect of PDT and SDT using ATX-70.[19] The growth of subcutaneously implanted murine squamous cell carcinomas was significantly suppressed by laser light irradiation immediately followed by ultrasound insonation when ATX-70 was injected 24 h before treatment. Histological changes showed that the combination therapy of PDT and SDT could induce tumor necrosis 2–3 times as deep as in either PDT alone or SDT alone. The combination of PDT and SDT with ATX-70 could be very useful for treatment of non-superficial tumors.

In this study, we used subcutaneously implanted murine Colon 26 carcinoma. It is very interesting to evaluate the antitumor effect and side effect of SDT with ATX-70 in a metastatic tumor system. Yumita *et al.* have already demonstrated a significant antitumor activity on Colon 26 implanted in kidney.[20] Further investigation of the antitumor effect and side effect of SDT with ATX-70 in metastatic liver or lung tumor models is needed.

In summary, we examined the behavior of ATX-70 in tumor-bearing mice, and estimated the distribution of ATX-70 in tumor tissue in comparison to normal tissues in order to predict the treatment effect as well as the possibility of adverse effects. Our findings have therapeutic implications for the planning of PDT or SDT with ATX-70. The pharmacokinetic method based on the compartment model that distinguishes between plasma and tissue which we have described in this paper should also be helpful in determining the best treatment plans for other agents.

ACKNOWLEDGMENTS

We thank Ms. Izumi Maruyama of Toyo Hakka Kogyo for providing ATX-70 and for useful advice.

(Received February 9, 2001/Revised June 5, 2001/Accepted June 19, 2001)

REFERENCES

1) Dougherty, T. J., Grindery, G. B., Weishaupt, K. R. and Boyle, D. G. Photoradiation therapy. II. Cure of animal tumors with hematoporphyrin and light. *J. Natl. Cancer Inst.*, **55**, 115–121 (1975).
2) Hayata, Y., Kato, H., Konaka, C., Ono, J. and Takizawa, N. Hematoporphyrin derivative and laser photoradiation in the treatment of lung cancer. *Chest*, **81**, 269–277 (1982).
3) Yumita, N., Nishigaki, R., Umemura, K. and Umemura, S. Hematoporphyrin as a sensitizer of cell-damaging effect of ultrasound. *Jpn. J. Cancer Res.*, **80**, 219–222 (1989).
4) Umemura, S., Yumita, N., Nishigaki, R. and Umemura, K. Mechanism of cell damage by ultrasound in combination with hematoporphyrin. *Jpn. J. Cancer Res.*, **81**, 962–966 (1990).
5) Yumita, N., Nishigaki, R., Umemura, K. and Umemura, S. Synergistic effect of ultrasound and hematoporphyrin on sarcoma 180. *Jpn. J. Cancer Res.*, **81**, 304–308 (1990).
6) Yumita, N., Nishigaki, R., Umemura, K., Morse, P. D., Swartz, H. M., Cain, C. A. and Umemura, S. Sonochemical activation of hematoporphyrin; an ESR study. *Radiat. Res.*, **138**, 171–176 (1994).
7) Nakajima, S., Maeda, T., Omote, Y., Hayashi, H., Yamazaki, K., Kubo, Y., Takemura, S., Shindo, Y. and Sakata, I. Tumor localizing Ga-porphyrin complex (ATX-70) as a new photosensitizer excited with YAG-laser. *J. Jpn. Soc. Laser Med.*, **10**, 225–228 (1989).
8) Umemura, S., Yumita, N. and Nishigaki, R. Enhancement of ultrasonically induced cell damage by a gallium-porphyrin complex, ATX-70. *Jpn. J. Cancer Res.*, **84**, 582–588 (1993).
9) Gomer, C. J. and Dougherty, T. J. Determination of [^{3}H] and [^{14}C] hematoporphyrin derivative distribution in malignant and normal tissue. *Cancer Res.*, **39**, 146–151 (1979).
10) Bellnier, D. A., Ho, Y.-K., Pandey, R. K., Missert, J. R. and Dougherty, T. J. Distribution and elimination of Photofrin II in mice. *Photochem. Photobiol.*, **50**, 221–228 (1989).
11) Yumita, N., Sasaki, K., Umemura, S. and Nishigaki, R. Sonodynamically induced antitumor effect of a gallium-porphyrin complex, ATX-70. *Jpn. J. Cancer Res.*, **87**, 310–316 (1996).
12) Yamaoka, K., Nakagawa, T. and Uno, T. Application of Akaike's information criterion (AIC) in the evaluation of linear pharmacokinetic equations. *J. Pharmacokinet. Biopharm.*, **6**, 165–175 (1978).
13) Kessel, D. Porphyrin-lipoprotein association as a factor in porphyrin localization. *Cancer Lett.*, **33**, 183–188 (1986).
14) Jori, G., Beltramini, E., Reddi, B., Salvato, A., Pagnan, L., Ziron, L., Tomio, L. and Tsanov, T. Evidence for a major role of plasma lipoproteins as hematoporphyrin carriers *in vivo*. *Cancer Lett.*, **24**, 291–297 (1984).
15) Barel, A., Jori, G., Perin, P., Pagnan, A. and Biffanti, S. Role of high-, low- and very density lipoproteins in the transport and tumor-delivery of hematoporphyrin. *Cancer Lett.*, **32**, 145–150 (1986).
16) Norata, G., Canti, G., Ricci, L., Nicolin, A., Trezzi, E. and Catapano, A. L. *In vivo* assimilation of low density lipoprotein by a fibrosarcoma tumor line in mice. *Cancer Lett.*, **25**, 203–208 (1984).

17) Vitols, S., Angelin, B., Ericksson, S., Gahrton, G., Juliusson, G., Masquelier, M., Paul, C., Peterson, C., Rudling, C., Söderbery-Reid, K. and Tidefelt, U. Uptake of low density lipoproteins by human leukemic cells *in vivo*: relation to plasma lipoprotein levels and possible relevance for selective chemotherapy. *Proc. Natl. Acad. Sci. USA*, **87**, 2598–2602 (1990).
18) Sasaki, K., Yumita, N., Nishigaki, R. and Umemura, S. Antitumor effect sonodynamically induced by focused ultrasound in combination with Ga-porphyrin complex. *Jpn. J. Cancer Res.*, **89**, 452–456 (1998).
19) Jin, Z., Miyoshi, N., Ishiguro, K., Umemura, S., Kawabata, K., Yumita, N., Sakata, I., Takaoka, K., Udagawa, T., Nakajima, S., Tajiri, H., Ueda, K., Fukuda, M. and Kumakiri, M. Combination effect of photodynamic and sonodynamic therapy on experimental skin squamous cell carcinoma in C3H/HeN mice. *J. Dermatol.*, **27**, 294–306 (2000).
20) Yumita, N., Sasaki, K., Umemura, S., Yukawa, A. and Nishigaki, R. Sonodynamically induced antitumor effect of gallium-porphyrin complex by focused ultrasound on experimental kidney tumor. *Cancer Lett.*, **112**, 79–86 (1997).